Journal of Molecular Catalysis A: Chemical 319 (2010) 46–51

Contents lists available at ScienceDirect

Journal of Molecular Catalysis A: Chemical

journal homepage: www.elsevier.com/locate/molcata

Novel thermally stable phosphorus-doped TiO_2 photocatalyst synthesized by hydrolysis of $TiCl_4$

Renyang Zheng, Ying Guo, Chen Jin, Jinglin Xie, Yuexiang Zhu*, Youchang Xie

Beijing National Laboratory for Molecular Science, State Key Laboratory for Structural Chemistry of Unstable and Stable Species, College of Chemistry and Molecular Engineering, Peking University, Beijing 100871, China

ARTICLE INFO

Article history:
Received 21 July 2009
Received in revised form
24 November 2009
Accepted 26 November 2009
Available online 2 December 2009

Keywords:
Titania
Phosphorus
Photocatalysis
Thermal stability

ABSTRACT

A novel thermally stable phosphorous-doped TiO_2 has been successfully synthesized by liquid hydrolysis of $TiCl_4$ with ammonia, with hypophosphorous acid as the precursor of the dopant. The materials were characterized by X-ray diffraction, transmission electron microscopy, differential thermal analysis–thermogravimetry, N_2 physical adsorption at 77 K, X-ray photoelectron spectroscopy and point of zero charge determination. It was found that increased calcination temperature gave an improvement of the anatase crystallinity and an enrichment of phosphorus species on the titania surface. The increased surface P content led to a linear enhancement of the specific adsorption capacity of methylene blue (MB) because of the Coulombic attractive force between the cationic dye and the negatively charged P-doped TiO_2 surface. Importantly, the P-doped anatase TiO_2 was stable even after calcination at 900 °C for 4 h, much more stable than the sample by the sol–gel method. This may be attributed to the partial transformation of amorphous titania to anatase during the hydrolysis of $TiCl_4$. Photocatalytic tests showed that the P-doped TiO_2 retained its high specific activity for the degradation of MB even after calcination at temperatures of 700–900 °C.

1. Introduction

Photocatalytic decomposition of organic pollutants on titania surfaces has attracted much interest for decades, with respect to both fundamental research and potential practical applications [1,2]. Titania has been widely investigated as one of the most promising heterogeneous photocatalysts in this field, because of its high photocatalytic activity, resistance to photocorrosion, photostability, low cost and non-toxicity. Titania exists in three different forms: anatase, rutile, and brookite, of which anatase generally shows the best photocatalytic activity and antibacterial performance [3–6]. Without any modification, transformation of anatase to rutile usually occurs at 500–700 °C [5,7]. The preparation of photocatalytic films on ceramic surfaces usually needs calcination at relatively high temperature (above 700 °C), which can lead to sintering and phase transformation and a consequent decrease in photocatalytic activity as well as cracking of the film. Thermally stable anatase TiO_2 with high photocatalytic activity may avoid the above deficiencies to form crack-free film with high photocatalytic performance.

To improve the thermal stability and photocatalytic activity, titania has been modified with La_2O_3 [7], ZrO_2, SiO_2 [8], trifluoroacetic acid [4], urea [5] and sulfur [9,10]. Among the various methods, modification of TiO_2 by phosphorus seems to be a promising approach [11–16]. Korosi et al. prepared phosphate-modified titania by phosphoric acid treatment of amorphous titania, during which process the thermal stability and photocatalytic activity of titania were enhanced [12]. Yu synthesized P-doped TiO_2 through hydrolysis and condensation of $Ti(OC_2H_5)_4$ with H_3PO_4 addition, and found that P-doped TiO_2 with a P/Ti atomic ratio of 0.03, calcined at 800 °C, caused efficient photocatalytic degradation of MB under UV irradiation [13]. We have recently synthesized P-doped titania with good photocatalytic performance by a modified sol–gel method from hypophosphorous acid and tetrabutyl titanate; the optimal calcination temperature was about 500 °C [17–19]. However, the work on P-modified titania has been generally done via a sol–gel method with organic titanate as precursor [11–13,17–19]. Fan et al. prepared phosphated mesoporous TiO_2 by an evaporation-induced self-assembly approach from $TiCl_4$ and H_3PO_4, and found that phosphorus improves the thermal stability. However, they mentioned only the photocatalytic activity of a sample calcined at 400 °C [14]. In the present work, we prepared P-doped TiO_2 by hydrolysis of $TiCl_4$ instead of the sol–gel method from tetrabutyl titanate. The results showed that the photocatalytic activity of TiO_2 was further enhanced, and the optimal calcination temperature was up to 700 °C. More importantly, thus prepared P-doped TiO_2 retained its high specific photocatalytic activity even after calcination at

* Corresponding author. Tel.: +86 10 62751703; fax: +86 10 62751708.
E-mail address: zhuyx@pku.edu.cn (Y. Zhu).

1381-1169/$ – see front matter © 2009 Elsevier B.V. All rights reserved.
doi:10.1016/j.molcata.2009.11.019

higher temperature (700–900 °C). In addition, the preparation strategy applied here can reduce the cost and avoid pollution by organic solvent [20]. Based on various physicochemical characterization techniques, a better understanding of the novel thermal stability and superior adsorption capacity of P-doped TiO_2 was obtained.

2. Experimental

2.1. Catalyst preparation

The P-doped TiO_2 was prepared by liquid hydrolysis of $TiCl_4$ with ammonia, with hypophosphorous acid as the precursor of the dopant. A typical synthesis procedure for P-doped TiO_2 was as follows. In an ice water bath, hypophosphorous acid (0.18 mL) was dissolved in 100 mL of deionized water and the solution was stirred magnetically for 10 min, and then 10 mL $TiCl_4$ was added, giving a nominal P:Ti atomic ratio of 0.01. The mixture was stirred for 30 min and a 25% ammonia solution was added dropwise to the solution until the pH of the mixture reached 5.5. A white precipitate was observed immediately. After aging at room temperature for 24 h, the precipitate was washed repeatedly with deionized water until no Cl^- ion was detected by adding 1 mol L^{-1} silver nitrate solution to the filtrate. The solid was then washed with ethanol and dried in air at 70 °C for about 1 day. The solid was ground to a fine powder to give a fresh sample followed by calcination at a given temperature for 4 h, to obtain P-doped titania TP-T, where *T* stands for the calcination temperature. For comparison, pure TiO_2 was prepared by the same procedure without the addition of hypophosphorous acid, whereas TP-sol-fresh (fresh sample dried at 100 °C) and TP-sol-600 (TP-sol-fresh calcined at 600 °C) were prepared by a modified sol–gel method from hypophosphorous acid and tetrabutyl titanate as reported previously [19].

2.2. Characterization

X-ray diffraction (XRD) patterns were collected with a Rigaku D/MAX-200 X-ray powder diffractometer with Ni-filtered Cu-Kα radiation at 40 kV and 100 mA. Transmission electron microscopy (TEM) images were obtained with a Philips FEI Tecnai F30 instrument. N_2 adsorption–desorption isotherms were determined at 77 K with a Micromeritics ASAP 2010 Analyzer. The samples were degassed in vacuum (10^{-3} Pa) for 2 h at 200 °C prior to adsorption measurements. Differential thermal analysis–thermogravimetry (DTA–TG) experiments were also carried out to monitor crystallization behavior using a Dupont model 1090 apparatus, from room temperature to 700 °C at a temperature-ramp rate of 10 °C min^{-1} in an air flow of 100 mL min^{-1}, using α-Al_2O_3 as reference. X-ray photoelectron spectroscopy (XPS) measurements were performed with a Kratos Axis Ultra System with monochromatic Al Kα X-rays (1486.6 eV), operated at 14 kV and 14 mA (emission current) in a chamber with base pressure approximately 10^{-8} Pa. All spectra were calibrated to the binding energy of the adventitious C1s peak at 284.8 eV. For depth profile experiments, the powdered sample was pressed into a thin disk 10 mm in diameter under a pressure of 15 MPa, and fitted on a rotatable stub for Ar^+ etching (at 4 kV). The sputtering rate was about 2 nm min^{-1} in terms of depth, with Ta_2O_5 film as a reference standard. The pH of the point of zero charge (PZC) of the samples was determined by mass titration [21,22]. This procedure involves finding the asymptotic value of the pH of an oxide/water suspension as the oxide mass content is increased. Varying amounts of samples (typical values of oxide/water by weight were 0.1, 1, 5, 10, 20 and 30%) were added to water, then ultrasonically dispersed for half an hour. The resulting pH was measured after equilibration for 1 day.

2.3. Photocatalytic activity test

The photocatalytic degradation of methylene blue (MB, $C_{16}H_{18}N_3S$) was chosen as a probe reaction [17]. In a typical experiment, 50.0 mg of the photocatalyst powder was dispersed in 200 mL aqueous MB solution (1.2×10^{-5} mol L^{-1}). The solutions were illuminated with a 6 W medium-pressure mercury lamp with main emission peak at 254 nm. The photocatalytic activity of the catalysts was tested after magnetic stirring for 1 h in darkness to achieve adsorption–desorption equilibrium. The concentration of MB was measured at 665 nm (λ_{max} for MB) by UV–vis spectroscopy. To evaluate the mineralization of MB over the photocatalysts, the total organic carbon (TOC) was determined by a TOC analyzer (TOC-V CPN, Shimadzu). In the TOC determination, 200 mL MB solution (5.0×10^{-5} mol L^{-1}) containing 50.0 mg of the catalyst was illuminated with a 100 W high-pressure mercury lamp with main emission peak at 365 nm. At each time interval, aliquots of MB solution were filtered through a 0.22 μm membrane (Satorius) and the filtrate was immediately subjected to the TOC analysis.

3. Results and discussion

3.1. Effect of P-doping on the thermal stability of anatase

The XRD patterns of pure and P-doped TiO_2 calcined at different temperatures are shown in Fig. 1, panels A and B, respectively. Only the diffraction peaks of the anatase form of TiO_2 can be observed in the XRD pattern of T-500, while a weak peak at around 27.5° appears in the pattern of T-600, indicating the formation of rutile at a temperature as low as 600 °C for pure TiO_2. By contrast, P-doped titania persisted as a pure anatase phase in the calcination temperature range of 500–900 °C, showing that the phase transformation of anatase to rutile was greatly retarded by P-doping. The average crystal sizes were calculated by using the Scherrer equation; the results are listed in Table 1. At the same calcination temperature, the crystal size of P-doped titania was substantially smaller than that of pure TiO_2. By investigating a series of doped titanias, Reidy et al. found that anatase is a metastable phase below a critical particle size of around 45 nm, regardless of the dopant [23]. Our crystal size data in Table 1 seem to fit well the critical size mechanism for the anatase to rutile transformation. Thus the P species may exist on grain boundary and act as hindrance to particle growth during calcination, inhibiting the phase transformation of anatase to rutile [24].

A TEM image was obtained to give more information about the morphology and particle size of P-doped TiO_2 (Supplementary material, Fig. S1). The representative image of TP-700 shows an average size of ~20 nm, which is in general agreement with the results from XRD.

Nitrogen adsorption–desorption isotherms were used for texture analysis (Supplementary material, Fig. S2). The observed type IV hysteresis loops in N_2 adsorption–desorption isotherms are characteristic of mesoporous structures. For the samples calcined at the same temperature, P-doped titania had smaller pore diameter and narrower pore size distribution than that of pure titania. The difference was more significant for the samples calcined at 700 °C. The most probable pore diameters centered at 17 nm (T-500), 32 nm (T-700), 7.7 nm (TP-500), and 15 nm (TP-700). The pore size distribution of T-700 became very broad, whereas TP-700 still retained a relatively narrow pore size distribution. The Brunauer–Emmett–Teller surface areas of the samples are summarized in Table 1. The surface areas of the samples increased from 79 m^2 g^{-1} for T-500 to 158 m^2 g^{-1} for TP-500. When calcined at 700 °C, the surface area of pure TiO_2 decreased drastically to 12 m^2 g^{-1}, whereas that of TP-700 was 59 m^2 g^{-1}. The decrease of surface area with increasing calcination temperature was much

Table 1
Summary of physicochemical and photocatalytic properties of samples.

Samples	Crystal size (nm)[a]		S_{BET} ($m^2\ g^{-1}$)	Adsorption capacity of MB (%)[b]	k_{app} ($10^{-3}\ min^{-1}$)
	Anatase	Rutile			
T-500	14.6		79	2.3	5.6
T-600	26.8 (88%)[c]	45.5 (12%)	34	3.8	6.8
T-700	(~2%)	61.1 (98%)	12	3.7	2.0
TP-500	10.5		158	4.3	21
TP-600	12.4		137	14.8	38
TP-700	18.9		59	22.0	57
TP-800	29.9		31	30.0	27
TP-900	37.0		21	23.4	17

[a] The average crystal size of TiO_2 was determined by the broadening of XRD peaks by Scherrer equation.
[b] The adsorption capability is represented by the percentage of MB adsorbed by photocatalyst during 1 h of adsorption–desorption equilibrium.
[c] The phase content of TiO_2 was obtained from the following formulas: $W_R = 1/[1 + 0.884(A_A/A_R)]$, $W_A = 1 - W_R$, where W_A and W_R are the content of anatase and rutile, respectively, A_A and A_R represent the diffraction intensity of anatase (101) and rutile (110).

smaller for P-doped TiO_2 than for pure titania. Clearly P-doping can stabilize the TiO_2 framework and increase the surface area.

Recently, Periyat et al. reported a thermally stable sulfur-doped anatase TiO_2 which showed 100% anatase at 800 °C and 20% anatase at 900 °C (with surface area 6.1 $m^2\ g^{-1}$) [6]. Previously, using tetrabutyl titanate as precursor, we synthesized by a sol–gel method P-doped TiO_2 containing 97% anatase, with surface area of 10 $m^2\ g^{-1}$ [19]. This might be due to the defects produced by excess hydroxyl and organic impurities in the amorphous titania prepared by the sol–gel method [25]. It should be emphasized that our current P-doped TiO_2 calcined at 900 °C retained the anatase content of 100% and a relatively high surface area (21 $m^2\ g^{-1}$). Evidently, P-doped TiO_2 prepared by hydrolysis of $TiCl_4$ shows superior thermal stability.

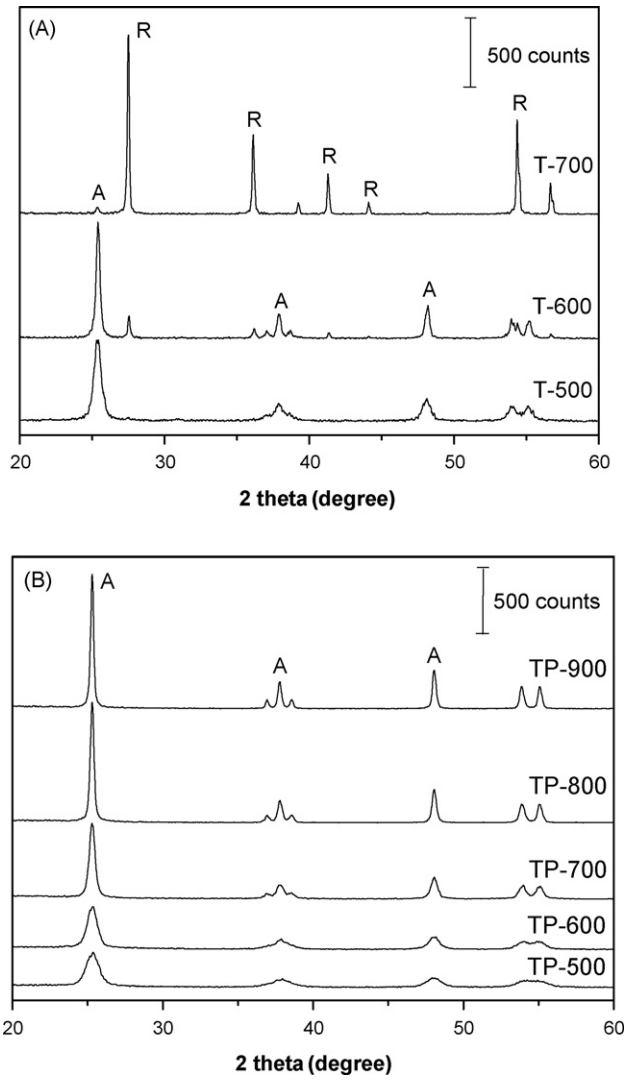

Fig. 1. XRD patterns of (A) T and (B) TP calcined at different temperatures. A and R denote anatase and rutile, respectively.

To investigate the origin of the thermal stability, DTA studies were performed on T and TP fresh powders (Fig. 2). Similar exothermic peaks around 270 °C were observed for the T and TP fresh powders: those peaks were attributed to thermal decomposition of residual ethanol from the washing process [19]. Another exothermic peak was observed at 468 °C for T fresh powders due to the formation of anatase. By contrast, TP fresh powders showed only two broad and weak exothermic peaks between 400 and 450 °C. The peak temperature was lower than those for T-sol-fresh and TP-sol-fresh samples prepared by the sol–gel method [19]. To understand the different exothermic peaks of anatase formation, XRD patterns of four fresh powders were obtained, as shown in Fig. 3. TP fresh powder (TP-fresh) showed weak diffraction peaks of anatase, whereas the other three fresh samples were amorphous. This indicates that hypophosphorous acid (P precursor) and H^+ (from the hydrolysis of $TiCl_4$) may play a catalytic role in the transformation of amorphous titania to anatase during the liquid hydrolysis of $TiCl_4$, as reported by Li et al. [26]. Anatase formed during hydrolysis can act as a crystallization seed, leading to the transformation of amorphous titania to anatase at a lower temperature. The fresh sample containing anatase seed should have higher resistance to sintering than the amorphous sample. This is probably the main reason for the superior thermal stability of P-doped TiO_2 prepared

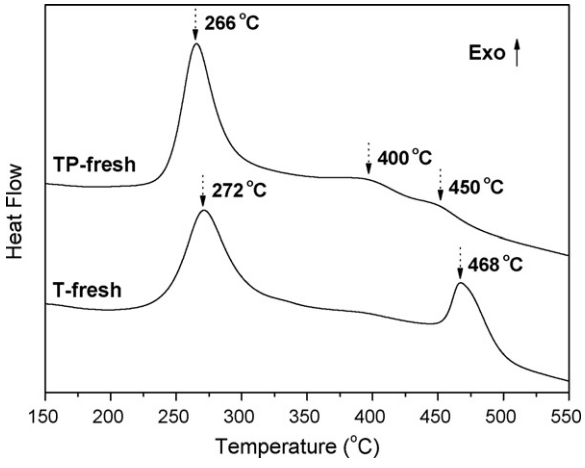

Fig. 2. DTA curves of T and TP fresh powders dried at 70 °C.

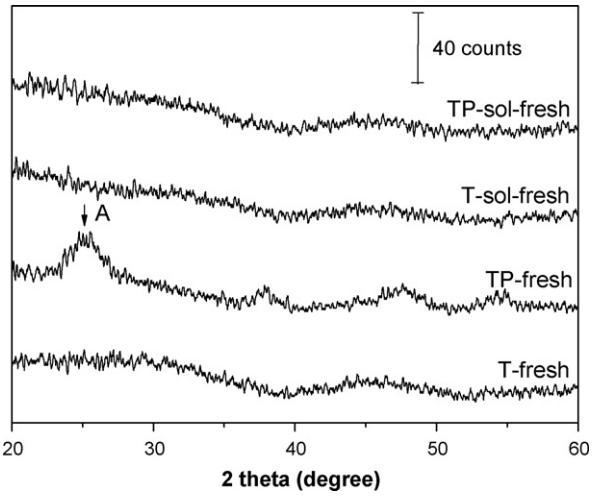

Fig. 3. XRD patterns of four fresh powders (TP-sol-fresh was a fresh sample dried at 100 °C and prepared by a sol–gel method from hypophosphorous acid and tetrabutyl titanate).

by hydrolysis of $TiCl_4$ compared to that prepared by the sol–gel method.

3.2. Relationship between surface P content and adsorption capacity of titania

P 2p XPS spectra were measured to investigate the chemical state and surface content of P in the samples. The P $2p_{3/2}$ binding energy of TP-700 was 133.4 eV, as previously reported [27,28], suggesting that P in the sample exists in the pentavalent oxidation state (P^{5+}). The doped P atoms probably replaced part of the Ti^{4+} in the TiO_2 lattice, in the form of a Ti–O–P linkage as reported in our previous work [19]. The preparation process in the current work provides further evidence. After aging of the precipitate suspension, the precipitate was washed repeatedly, during which Cl^- ion was removed but the P species was retained. In our previous work [29], pure TiO_2 was prepared by hydrolysis of $Ti(SO_4)_2$ and ammonia; SO_4^{2-} ion was removed during the washing process. Consequently, the fact that P species could not be removed confirmed formation of stable Ti–O–P linkages.

The surface P content (P/Ti atomic ratio) was determined from the areas of the P 2p and Ti 2p peaks considering the relative sensitivity factors. The data plotted in Fig. 4 show increasing enrichment

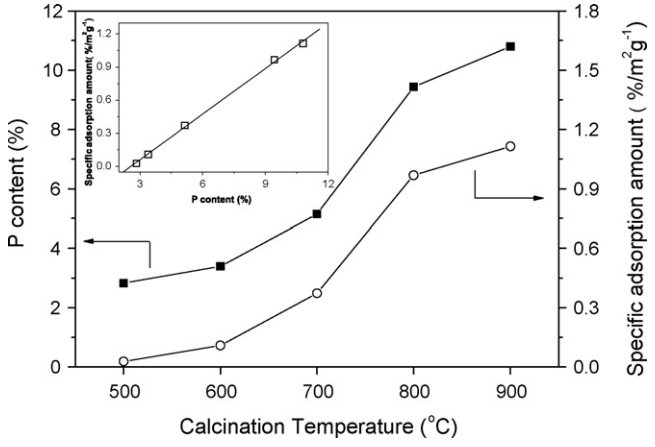

Fig. 4. The dependence of surface P content (solid squares) and specific adsorption capacity for MB (open circles) on calcination temperature of TP. The inset shows the linear relationship of specific adsorption capacity and surface P content.

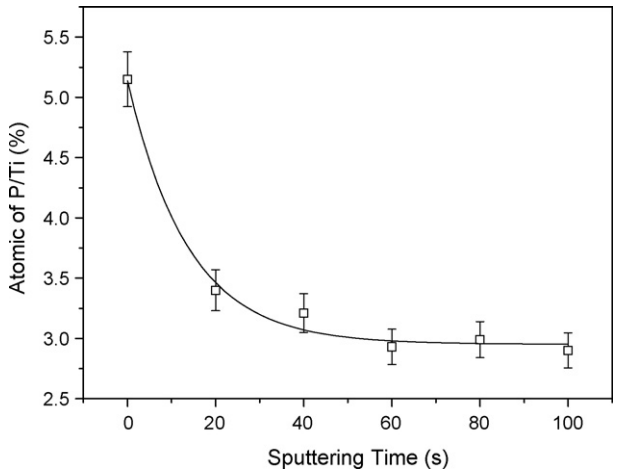

Fig. 5. Depth profile of P in TP-700 after Ar^+ etching.

of P species on the TiO_2 surface with increasing calcination temperature. This trend can be attributed to transfer of P species from the bulk network to the surface of titania during high temperature calcination. To obtain further information about the P depth profile in TiO_2 particles, XPS spectra of TP-700 after Ar^+ ion etching for different times were obtained. The results (Fig. 5) show a clear trend of P content decreasing from 5.1% at the surface to a steady value of 3.0% in the bulk, in the first 30 s of sputtering. These results indicate that P atoms were incorporated into the bulk phase of TiO_2 [30]. Considering the sputtering speed of 2 nm min^{-1}, we conclude that the P species were mainly enriched in a 1 nm surface layer. This kind of depth distribution has an influence on the adsorption capacity of TiO_2, as discussed below.

Adsorption is an important step in the photocatalytic process [31]. The adsorption capacity is represented by the percentage of MB adsorbed by photocatalyst during 1 h of adsorption–desorption equilibrium. The results are listed in Table 1. Generally speaking, samples with larger surface area have a stronger adsorption capacity under the same conditions. Hence, it is easy to understand that P-doped TiO_2 showed a larger capacity for adsorption of MB than undoped TiO_2 calcined at the same temperature. However, for P-doped TiO_2 the surface area decreased but adsorption capacity was greatly increased with increasing calcination temperature. To avoid the influence of surface area, the specific capacity for adsorption of MB was calculated and plotted in Fig. 4, which showed a linear relationship with surface P content.

The pH of the point of zero charge (PZC), determined by mass titration, was expected to elucidate the origin of the relationship between the surface P content and adsorption capacity. The pH of an aqueous suspension of an oxide depends on the oxide/water ratio. On addition of excess powder, the suspension pH often approaches a steady limit value that is a reasonable estimate of the PZC for the oxide [21,22]. Fig. 6A shows typical plots of pH versus catalyst/water mass percentage for pure and P-doped TiO_2. When the catalyst/water mass percentage was higher than 10%, there was no significant decrease in pH with further addition of solid. The steady limit values of pH, i.e. PZC values, were 5.7, 3.8, and 3.1 for T-500, TP-500 and TP-700, respectively. The PZC value determined for pure TiO_2 was consistent with other reports [32]. P-doping of TiO_2 calcined at 500 °C reduced the PZC from 5.7 to 3.8. Interestingly, the PZC for TP-500 (3.8) decreased to 3.1 for TP-700, whereas that of pure TiO_2 showed almost no difference between 500 and 700 °C (the data points for T-700 were omitted from the figure for clarity). These results indicate that surface acidity was enhanced when P-doped TiO_2 was calcined at higher temperature. To confirm the influence of calcination temperature on the PZC of P-doped TiO_2 we

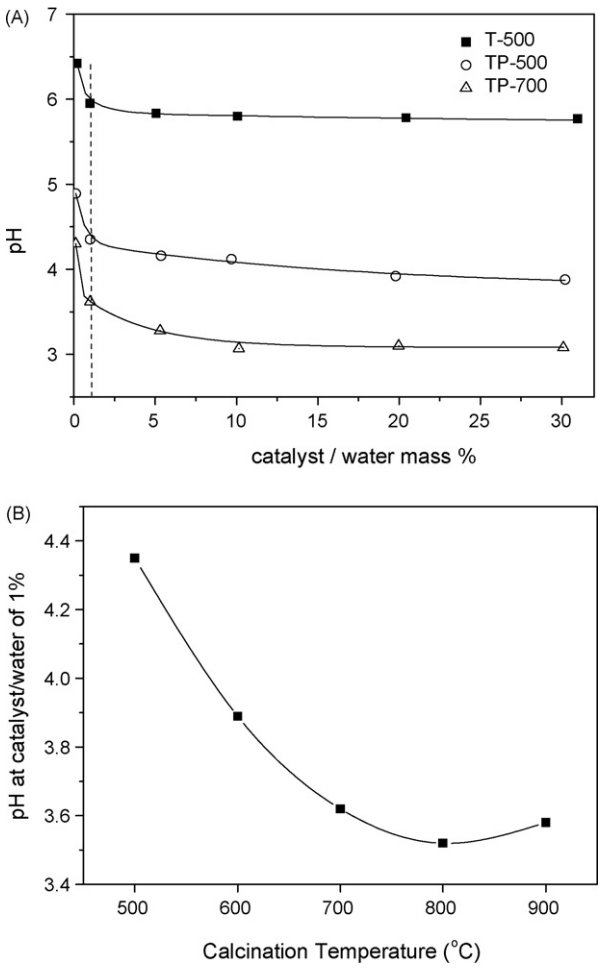

Fig. 6. (A) Plot of pH versus catalyst/water mass percentage for T and TP; (B) the dependence of pseudo-PZC on calcination temperature of TP.

measured the pseudo-PZC which is represented by the pH at catalyst/water mass percentage of 1% (indicated by the broken line in Fig. 6A). The results are shown in Fig. 6B. The pseudo-PZC value can reveal the trend in the PZC, and it is apparent that increasing calcination temperature enhanced the surface acidity, thereby reducing the PZC of P-doped TiO_2.

Since MB is a cationic dye (the molecular structure shown in Fig. 7A), adsorption of MB on TiO_2 is greatly influenced by the ionization state of the titania surface [33,34]. As illustrated in Fig. 7B, when the pH of the suspension is higher than the PZC of TiO_2 the surface becomes negatively charged, and vice versa when pH is lower than the PZC [35]. Because we did not control the pH of the photocatalytic reaction, it was nearly neutral for the adsorption process. The pH of the aqueous dispersion (~7) was much higher than the PZC of P-doped TiO_2 (3–4), so an attractive force between MB cationic dye and the negatively charged P-doped TiO_2 surface would favor the adsorption of MB on the surface. Thus the increase in specific adsorption capacity with calcination temperature is attributed to enrichment of surface P content of P-doped TiO_2 after calcination, which leads to the reduction of the PZC.

3.3. Photocatalytic property

The kinetics of the MB photocatalytic degradation was analyzed as previously reported [17]. The concentration of MB, denoted by c, decreased exponentially in first order with reaction time in the presence of various catalysts under UV-illumination (Supplementary material, Fig. S3), suggesting a pseudo-first order

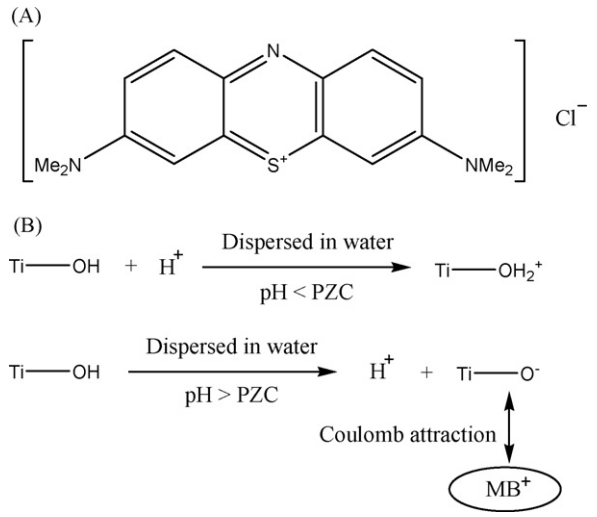

Fig. 7. (A) Molecular structure of methylene blue (MB); (B) schematic representation of MB adsorption on titania by Coulombic attraction.

reaction [34,36]. Apparent reaction rate constants k_{app} were deduced from linear fits of $\ln(c_0/c)$ versus reaction time and are summarized in Table 1. Compared with pure TiO_2, the P-doped TiO_2 samples showed much higher photocatalytic activity. The apparent first order rate constant, k_{app} of TP-700 was 57×10^{-3} min^{-1}, which is 10-fold higher than that of pure TiO_2. It has been proved in previous work that P-doped TiO_2 prepared by a sol–gel method has a higher surface area and smaller crystalline size than pure TiO_2, leading to enhancement of its photocatalytic activity [17]. Considering this point of view, it is easy to understand the superior photocatalytic performance of P-doped TiO_2 compared with pure TiO_2.

Interestingly, the photocatalytic activity of P-doped TiO_2 calcined at elevated temperatures was greatly enhanced, even though the surface area was reduced. The rate constant of P-doped TiO_2 increased gradually with increasing calcination temperature up to about 700 °C and decreased at higher calcination temperatures. After calcination at 900 °C, the activity of P-doped TiO_2 was smaller, but its k_{app} was still 2.5 times higher than that of T-600. By contrast, the photocatalytic activity decreased greatly when the calcination temperature of pure TiO_2 was increased from 600 to 700 °C.

Photocatalytic activity depends on several factors, including phase composition, crystal size, crystallinity, surface area, nature of dopants and adsorption capacity [5,19]. To achieve a concise understanding of the effect of high temperature calcination, the specific rate constant obtained by division of k_{app} by surface area is plotted as a function of calcination temperature in Fig. 8. The specific rate constant of P-doped TiO_2 increased gradually with increasing calcination temperature up to about 700 °C and the high performance was maintained even after calcination at higher temperatures (700–900 °C). This phenomenon can be ascribed, on the one hand, mainly to improved crystallinity of anatase by high temperature treatment, as reported by Padmanabhan et al. [4] and Yu et al. [37]. The intensity of the XRD peak at 25.3° of TP-700 was 1.7 times higher than that of TP-sol-600, i.e. P-doped TiO_2 calcined at 600 °C prepared by the sol–gel method reported in our previous paper [19]. The rate constant for TP-700 was 1.6 times higher than that for TP-sol-600 (34×10^{-3} min^{-1}), which was the best photocatalyst in that series of P-doped TiO_2 materials. Consequently, the superior performance of P-doped TiO_2 prepared from $TiCl_4$ compared to the material prepared from tetrabutyl titanate may be mainly due to the increased crystallinity of anatase.

On the other hand, with increasing calcination temperature the enrichment of P species favored adsorption of MB cationic dye on

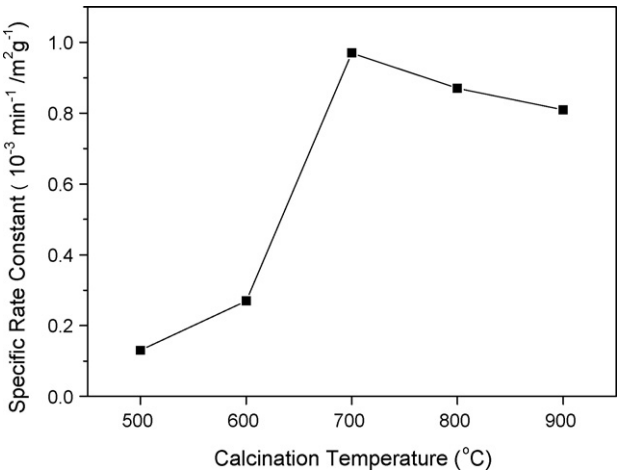

Fig. 8. The dependence of specific rate constants on calcination temperature of TP.

P-doped TiO_2 (Fig. 4). To understand the influence of adsorption on photocatalytic performance, it is necessary to briefly review the mechanism of MB photocatalytic degradation. In a typical photocatalysis process, when a photon with a proper energy matches or exceeds the band gap E_g of TiO_2, an electron–hole (e^-/h^+) pair is created within the TiO_2 particles by ejection of an electron from the valence band into the conduction band, leaving behind a hole in the valence band [1]. There are two oxidative agents in TiO_2: photogenerated holes h^+ and hydroxyl radicals $OH^\bullet$. As a cationic dye, MB is difficult to attack by holes h^+ because of the repulsive Coulombic force. Hence hydroxyl radical attack is mainly responsible for MB degradation. Houas et al. investigated the photocatalytic degradation pathway of MB in water in detail [33]. They found that MB degradation mainly begins with cleavage of the $C–S^+=C$ functional group, which is adsorbed on the TiO_2 surface. Subsequently almost complete mineralization of carbon, and nitrogen and sulfur heteroatoms into CO_2, NH_4^+, NO_3^- and SO_4^{2-} takes place. The low PZC of P-doped TiO_2 favored high adsorption of MB by Coulombic attraction between MB^+ and $Ti–O^-$ sites, making the process of hydroxyl radical attack more facile, and as a result MB was effectively degraded.

Additionally, surface P species may act as trapping sites to capture the e^-, leading to more effective separation of light-generated e^-/h^+ pairs and enhancement of photocatalytic activity. The phenomenon has also been observed in transition metal supported TiO_2 [1,35], S-doped [38] and I-doped [39] TiO_2.

In order to evaluate the complete mineralization of MB over the catalysts, total organic carbon (TOC) was also measured (Supplementary material, Fig. S4). The results showed that the rate of mineralization is much lower than that of degradation as reported in the literature [40]. The TOC decreasing rate over P–TiO_2 was higher than that over the pure sample. However, the difference was not as obvious as for MB degradation shown in Supplementary material, Fig. S3. Further study on the mechanism is in progress.

4. Conclusion

P-doped TiO_2 with high photocatalytic activity and novel thermal stability has been prepared by a simple, low-cost and reproducible method. P-doping can greatly retard the phase transition of anatase to rutile. P-doped TiO_2 calcined at 900 °C retains 100% anatase and a high surface area of 21 $m^2\,g^{-1}$. Increased calcination temperature gives an improvement of the anatase crystallinity and an enhancement of adsorption capacity. The synergistic effect of P-doping and high temperature calcination leads to the excellent performance of P-doped TiO_2. The photocatalytic activity of P-doped titania calcined at 700 °C is 10-fold higher than that of pure TiO_2. The novel thermal stability and high photocatalytic performance of the P-doped TiO_2 makes it very promising for applications in the field of industrial manufacture of environmental protection photocatalysts, such as antibacterial self-cleaning building materials.

Acknowledgements

This work was supported by funding from the National Science Foundation of China (20973012 and JO630421), and the Major State Basic Research Development Program (Grant No. 2006CB806102).

Appendix A. Supplementary data

Supplementary data associated with this article can be found, in the online version, at doi:10.1016/j.molcata.2009.11.019.

References

[1] X. Chen, S.S. Mao, Chem. Rev. 107 (2007) 2891–2959.
[2] P. Periyat, D.E. McCormack, S.J. Hinder, S.C. Pillai, J. Phys. Chem. C 113 (2009) 3246–3253.
[3] O. Carp, C.L. Huisman, A. Reller, Prog. Solid State Chem. 32 (2004) 33–177.
[4] S.C. Padmanabhan, S.C. Pillai, J. Colreavy, S. Balakrishnan, D.E. McCormack, T.S. Perova, Y. Gun'ko, S.J. Hinder, J.M. Kelly, Chem. Mater. 19 (2007) 4474–4481.
[5] S.C. Pillai, P. Periyat, R. George, D.E. McCormack, M.K. Seery, H. Hayden, J. Colreavy, D. Corr, S.J. Hinder, J. Phys. Chem. C 111 (2007) 1605–1611.
[6] P. Periyat, S.C. Pillai, D.E. McCormack, J. Colreavy, S.J. Hinder, J. Phys. Chem. C 112 (2008) 7644–7652.
[7] J. Zhang, M.J. Li, Z.C. Feng, J. Chen, C. Li, J. Phys. Chem. B 110 (2006) 927–935.
[8] D.J. Reidy, J.D. Holmes, C. Nagle, M.A. Morris, J. Mater. Chem. 15 (2005) 3494–3500.
[9] G. Colon, M.C. Hidalgo, G. Munuera, I. Ferino, M.G. Cutrufello, J.A. Navio, Appl. Catal. B 63 (2006) 45–59.
[10] R. Gomez, T. Lopez, E. Ortis-Islas, J. Navarrete, E. Sanchez, F. Tzompanztzi, X. Bokhimi, J. Mol. Catal. A 193 (2003) 217–226.
[11] J.C. Yu, L.Z. Zhang, Z. Zheng, J.C. Zhao, Chem. Mater. 15 (2003) 2280–2286.
[12] L. Korosi, S. Papp, I. Bertoti, I. Dekany, Chem. Mater. 19 (2007) 4811–4819.
[13] H.F. Yu, J. Phys. Chem. Solids 68 (2007) 600–607.
[14] X.X. Fan, T. Yu, Y. Wang, J. Zheng, L. Gao, Z.S. Li, J.H. Ye, Z.G. Zou, Appl. Surf. Sci. 254 (2008) 5191–5198.
[15] X.Q. Chen, X.W. Zhang, Y.L. Su, L.C. Lei, Appl. Surf. Sci. 254 (2008) 6693–6696.
[16] D. Zhao, C.C. Chen, Y.F. Wang, H.W. Ji, W.H. Ma, L. Zang, J.C. Zhao, J. Phys. Chem. C 112 (2008) 5993–6001.
[17] L. Lin, W. Lin, J.L. Xie, Y.X. Zhu, B.Y. Zhao, Y.C. Xie, Appl. Catal. B 75 (2007) 52–58.
[18] L. Lin, R.Y. Zheng, J.L. Xie, Y.X. Zhu, Y.C. Xie, Appl. Catal. B 76 (2007) 196–202.
[19] R.Y. Zheng, L. Lin, J.L. Xie, Y.X. Zhu, Y.C. Xie, J. Phys. Chem. C 112 (2008) 15502–15509.
[20] M. Addamo, V. Augugliaro, A. Di Paola, E. Garcia-Lopez, V. Loddo, G. Marci, L. Palmisano, Colloids Surf. A 265 (2005) 23–31.
[21] S. Subramanian, J.S. Noh, J.A. Schwarz, J. Catal. 114 (1988) 433–439.
[22] A. Di Paola, G. Marci, L. Palmisano, M. Schiavello, K. Uosaki, S. Ikeda, B. Ohtani, J. Phys. Chem. B 106 (2002) 637–645.
[23] D.J. Reidy, J.D. Holmes, M.A. Morris, J. Eur. Ceram. Soc. 26 (2006) 1527–1534.
[24] F. Li, Y. Jiang, M. Xia, M. Sun, B. Xue, D. Liu, X. Zhang, J. Phys. Chem. C 113 (2009) 18134–18141.
[25] M.S.P. Francisco, V.R. Mastelaro, Chem. Mater. 14 (2002) 2514–2518.
[26] Y. Li, N.-H. Lee, D.-S. Hwang, J.S. Song, E.G. Lee, S.-J. Kim, Langmuir 20 (2004) 10838–10844.
[27] L. Lin, W. Lin, Y.X. Zhu, B.Y. Zhao, Y.C. Xie, Chem. Lett. 34 (2005) 284–285.
[28] Q. Shi, D. Yang, Z.Y. Jiang, J. Li, J. Mol. Catal. B 43 (2006) 44–48.
[29] L. Lin, W. Lin, Y.X. Zhu, B.Y. Zhao, Y.C. Xie, Y. He, Y.F. Zhu, J. Mol. Catal. A 236 (2005) 46–53.
[30] T. Ohno, M. Akiyoshi, T. Umebayashi, K. Asai, T. Mitsui, M. Matsumura, Appl. Catal. A 265 (2004) 115–121.
[31] F. Chen, J.C. Zhao, H. Hidaka, Res. Chem. Intermed. 29 (2003) 733–748.
[32] X.Z. Li, F.B. Li, C.L. Yang, W.K. Ge, J. Photochem. Photobiol. A 141 (2001) 209–217.
[33] A. Houas, H. Lachheb, M. Ksibi, E. Elaloui, C. Guillard, J.M. Herrmann, Appl. Catal. B 31 (2001) 145–157.
[34] T.Y. Zhang, T. Oyama, A. Aoshima, H. Hidaka, J.C. Zhao, N. Serpone, J. Photochem. Photobiol. A 140 (2001) 163–172.
[35] F. Kiriakidou, D.I. Kondarides, X.E. Verykios, Catal. Today 54 (1999) 119–130.
[36] M. Srinivasan, T. White, Environ. Sci. Technol. 41 (2007) 4405–4409.
[37] J.C. Yu, J.G. Yu, W.K. Ho, Z.T. Jiang, L.Z. Zhang, Chem. Mater. 14 (2002) 3808–3816.
[38] J.C. Yu, W. Ho, J. Yu, H. Yip, P.K. Wong, J. Zhao, Environ. Sci. Technol. 39 (2005) 1175–1179.
[39] S. Tojo, T. Tachikawa, M. Fujitsuka, T. Majima, J. Phys. Chem. C 112 (2008) 14948–14954.
[40] J. Yu, G. Dai, B. Huang, J. Phys. Chem. C 113 (2009) 16394–16401.